NJC

Accepted Manuscript

This is an *Accepted Manuscript*, which has been through the Royal Society of Chemistry peer review process and has been accepted for publication.

Accepted Manuscripts are published online shortly after acceptance, before technical editing, formatting and proof reading. Using this free service, authors can make their results available to the community, in citable form, before we publish the edited article. We will replace this *Accepted Manuscript* with the edited and formatted *Advance Article* as soon as it is available.

You can find more information about *Accepted Manuscripts* in the Information for Authors.

Please note that technical editing may introduce minor changes to the text and/or graphics, which may alter content. The journal's standard Terms & Conditions and the Ethical guidelines still apply. In no event shall the Royal Society of Chemistry be held responsible for any errors or omissions in this *Accepted Manuscript* or any consequences arising from the use of any information it contains.

ROYAL SOCIETY OF CHEMISTRY

www.rsc.org/njc

Kurnakov Institute of General and Inorganic Chemistry, Russian Academy of Sciences, Leninsky Prosp. 31, 119991 Moscow, Russian Federation. E-mail:ilyukhin@rambler.ru

†Electronic supplementary information (ESI) available: CIF files of the structural data for seven compounds and data collection and structure refinement statistics. CCDC 987443-987449 For ESI and crystallographic data in CIF or other electronic formats see DOI:

SUPRAMOLECULAR AGGREGATION OF YTTRIUM THIOCYANATE WITH 4,4'-BIPYRIDINE

Svetlana Petrosyants, Zhanna Dobrokhotova, Andrey Ilyukhin*, Vladimir Novotortsev

Abstract

The reaction of yttrium thiocyanate $[Y(H_2O)_5(NCS)_3]\cdot H_2O$ with 4,4'-bipyridine (bpy) was studied in various solvents. The complexes $[Y(H_2O)_3EtOH(bpy)(NCS)_3)]\cdot bpy$ (**1**), $\{(\mu\text{-}bpy)[Y(H_2O)_3(NCS)_3]_2\}\cdot 3bpy\cdot 2(i\text{-}PrOH)$ (**2**), and $[Hbpy]_2\{(\mu\text{-}bpy)[Y(H_2O)_3(NCS)_4]_2\}\cdot bpy$ (**3**) were isolated as the main phases (the former from ethanol, and the latter two from i-PrOH). Complex **3** formed also in MeCN and thf. Assemblies **1-3** were identified based on single-crystal and powder X-ray diffraction and IR spectroscopic data. Supramolecular aggregation in **1-3** occurs through OH…N(S) hydrogen bonds. Despite different compositions and arrangement of structural units, the crystal structures **1-3** are similar and consist of interpenetrating rectangular 3D networks. Thermal analysis showed that the decomposition of **1-3** occurs in a similar way. Coordinated water and alcohol molecules are eliminated at temperatures below 170 ºC; at temperatures above 230 ºC, the multistep elimination of bpy and decomposition of NCS take place. Photoluminescent characteristics of **1-3** provide evidence that bpy are involved in the energy transfer resulting in a long-wavelength shift of emission maxima.

Introduction

The design and construction of architectures having properties useful for the practical application as molecular sensors, luminescent materials, as well as in catalysis, adsorption, gas storage, and so on, hold a prominent place in supramolecular chemistry.[1] The use of metal ions and organic ligands for the preparation of hybrid metal-organic frameworks has considerable promise for designing such materials. Since the triply charged yttrium cation belongs to hard acids in terms of the HSAB concept, ligands containing hard donor atoms (N, O) or acido ligands (halides, pseudohalides) are preferable for this cation. The large ionic radius of Y^{3+}

combined with the predominantly electrostatic nature of the metal-ligand binding is responsible for the formation of compounds with coordination number (CN) from 4 to 9. The coordination and structural diversity of yttrium compounds is considered in detail in the review.[2]

Aromatic nitrogen heterocycles play a key role in the self-organization and design of macromolecular architectures. 4,4'-Bipyridine (bpy) is most commonly used in this area. This compound (1) is a ditopic ligand and can bridge between metal centers, (2) in the protonated form, can act as a counterion, (3) can serve as a guest occupying cavities in the structure, or (4) can be coordinated to a metal ion in a monodentate fashion. For example, in the structure of $[Y(crot)_3(H_2O)(bpy)_{1/2}]_n$, bpy molecules act as bidentate-bridging ligands and link dimeric yttrium polyhedra (CN 9) coordinated by chelating and bridging crotonate anions to form polymer chains.[3] The structure of $[Y(nip)_2][H_2(bpy)]_{0.5}$ (H_2nip is 5-nitroisophthalic acid) contains 1-D chains Y-O-C-O-Y linked by carboxylate ligands to form layers, wherein protonated diimine is not involved in the coordination and is located between the layers.[4] In the dimeric compound $[Y_2(Hca)_6(bpy)_2(H_2O)_2]\cdot 2bpy$, where H_2ca is 2-hydroxycinnamic acid, the dimerization occurs *via* carboxylate groups of Hca. These groups link two yttrium polyhedra (CN 8); one bpy molecule in each polyhedron is coordinated in a monodentate fashion and two other bpy molecules are in the solvation sphere. In this assembly, hydrogen bonds play a key role in the formation of a 3D supramolecular framework.[5] The supramolecular aggregation based on hydrogen bonding is typical also of the assembly $[Y(H_2O)_4(NCS)_3]\cdot 1.5$(18-crown-6), which was synthesized by the reaction of $[Y(H_2O)_5(NCS)_3].H_2O$ with 18-crown-6 in methanol.[6] Changes in the reaction conditions or the use of alternative solvent systems promote the appearance of new forms, and secondary interactions give rise to unusual and interesting structural motifs and polynuclear assemblies.[2,6]

It is known that the photoluminescence of metal thiocyanate complexes is due to fluorescence of the thiocyanate ion.[7] In assemblies with organic ligands, particularly, in those containing nitrogen-containing aromatic linkers, the fluorescence can be centered on organic linkers acting as antennas. Studies on the luminescence properties of *d*-metal thiocyanate complexes are scarce.[8, 9] The emission spectra of KSCN and the complex $[Y(H_2O)_5(NCS)_3]\cdot H_2O$ were broad and almost unstructured.[7] This suggests that the $S_1 \rightarrow S_0$ fluorescence of the SCN^- ion plays a key role in the luminescence of the complex $[Y(H_2O)_5(NCS)_3]\cdot H_2O$. In the luminescence spectra of complexes, the emission band is usually associated with the transition of the molecule from the excited (S_1) to the ground state (S_0). Fluorescence is determined by the following factors: (1) the nature of the central atom (metal), (2) the nature of the organic ligand, and (3) the molecular packing in the structure. It was of interest to investigate the effect of bipyridine on the fluorescence of thiocyanate supramolecular assemblies **1**-**3**.

In the present study, we investigated the reaction of yttrium thiocyanate $[Y(H_2O)_5(NCS)_3]\cdot H_2O$ with bpy in a series of solvents and isolated $[Y(H_2O)_3EtOH(bpy)(NCS)_3)]\cdot bpy$ (**1**) from ethanol, $\{(\mu\text{-bpy})[Y(NCS)_3(H_2O)_3]_2\}\cdot 3bpy\cdot 2(i\text{-PrOH})$ (**2**) and $\{Hbpy\}_2\{(\mu\text{-bpy})[Y(H_2O)_3(NCS)_4]_2\}\cdot bpy$ (**3**) from i-PrOH and from solutions in MeCN and thf. The assemblies were identified by X-ray diffraction. Their thermochemical behavior was studied, and the photoluminescent characteristics were determined.

Results and discussion

Self-assembly of the metal salts with 4,4 '-Bipyridine (bpy) leading to dimeric or polymeric compounds in which a ligand ditopnost realized. Supramolecular ensembles appear as a result of noncovalent binding, hydrogen bonding, π-π stacking or outer-sphere interactions of ligands with metal complexes. The aim of the present study was to investigate the role of medium (the nature of the solvent, pH, ratio of reagents) on aggregation of yttrium thiocyanate complexes with bpy. This implied the synthesis of supramolecular ensembles, reveal the influence of association and polymerization on structural features ensembles.

Consideration of the synthesis

Based on single-crystal and powder X-ray diffraction, IR spectroscopic, and elemental analysis data, the reaction of yttrium thiocyanate with bpy in the solvents used in the present study can be described by Scheme 1.

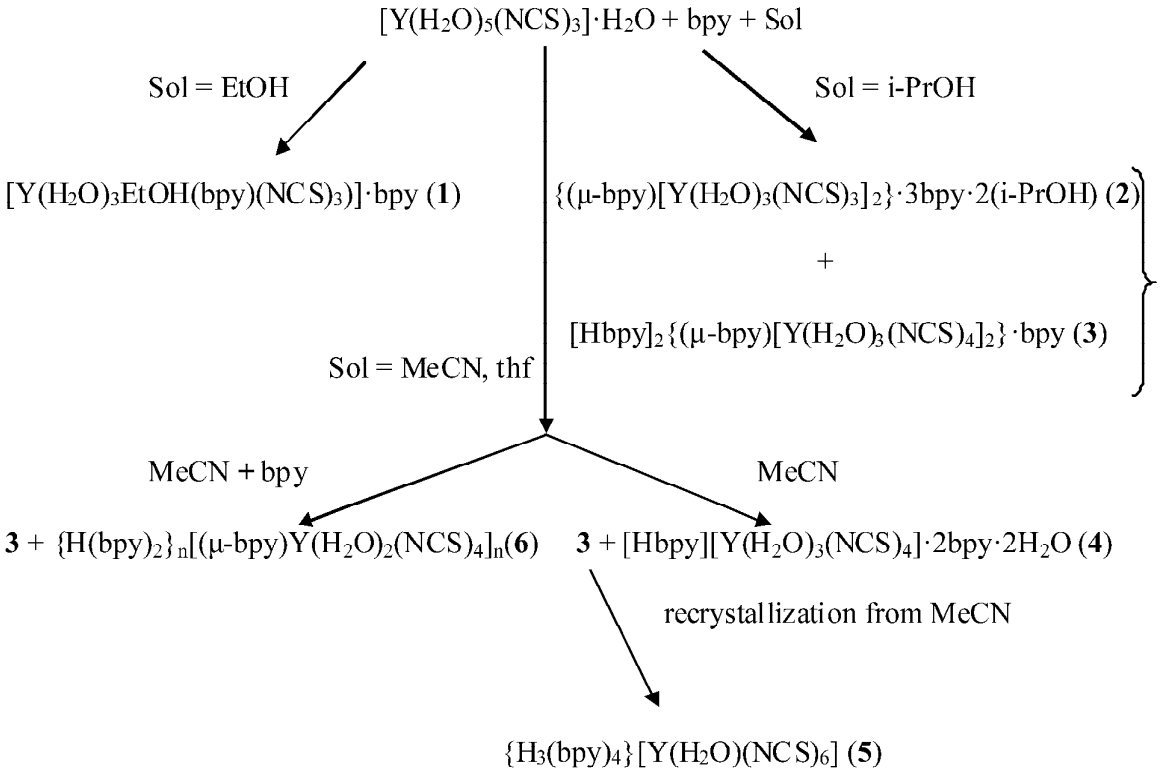

Scheme 1. Synthetic route to complexes

The reaction of yttrium thiocyanate with bpy in EtOH affords $[Y(H_2O)_3EtOH(bpy)(NCS)_3]\cdot bpy$ (**1**). Compound **1** with the ratio bpy : Y = 2 was isolated from ethanolic solutions, in which the initial bpy : Y ratio was varied from 1 to 4, an increase in the ratio resulting in a decrease in the purity of the product. Pure **1** (X-ray powder diffraction) was obtained from a solution with the ratio bpy : Y = 2. A relatively low yield (~50%) is attributed to high solubility of **1** in ethanol. In assembly **1**, one bpy molecule is coordinated in a monodentate fashion, whereas another bpy is a molecule of solvation. It is interesting that it is the bpy molecule rather than protolytic H_2O or EtOH molecules that is present in the solvation sphere. The assembly $\{(\mu\text{-bpy})[Y(H_2O)_3(NCS)_3]_2\}\cdot 3bpy\cdot 2(i\text{-PrOH})$ (**2**) was synthesized according to the following two procedures: by the treatment of **1** with i-PrOH (synthesis A) or by the direct reaction of yttrium thiocyanate with bpy in i-PrOH (synthesis B). The formation of **2** can be considered as the dimerization of **1** accompanied by elimination of EtOH from the coordination sphere and the change in the coordination mode of the bpy ligand from monodentate to bridging. It is noteworthy that the supramolecular assembly **2** contains two i-PrOH molecules along with three bpy molecules in the solvation sphere. It should be emphasized that the anionic dimeric assembly $[Hbpy]_2\{(\mu\text{-bpy})[Y(H_2O)_3(NCS)_4]_2\}\cdot bpy$ (**3**) was detected (X-ray powder diffraction) in i-PrOH regardless of the bpy : Y ratio. The formation of the latter assembly is determined by kinetic factors (see the Experimental section). Dimer **3** was isolated as the main phase also from solutions in MeCN and thf. Crystals of $[Hbpy][Y(H_2O)_3(NCS)_4]\cdot 2bpy\cdot 2H_2O$ (**4**) were obtained from the mother liquor of the reaction mixture in MeCN. The detection of crystals of **4** in the mother liquor indicates that the reaction proceeds through monomer **4** to dimer **3** accompanied by the change in the position of one bpy molecule, which is located in the outer sphere in **4**, whereas it acts as a bridge in **3**. This process is similar to the dimerization of molecular complexes **1** → **2** in going from ethanol to i-PrOH, which results in the change in the coordination mode of the bpy molecule from monodentate in **1** to bridging in **2.** The formation of **3** in solutions in thf occurs in a similar way. It should be noted that insoluble, predominantly amorphous, phases immediately precipitate from the reaction mixture in aprotic solvents (MeCN, thf), complex **3** being the main component. The recrystallization of **3** from acetonitrile afforded crystals of $\{H_3(bpy)_4\}[Y(H_2O)(NCS)_6]$ (**5**). An increase in the bpy : Y ratio in acetonitrile led to the formation of $\{H(bpy)_2\}_n[(\mu\text{-bpy})Y(H_2O)_2(NCS)_4]_n$ (**6**) as an impurity phase along with **3.**

Compounds **3 – 6** contain anionic moieties with four (**3 - 4** and **6)** or six (**5**) thiocyanate anions in the coordination sphere of yttrium, although the starting thiocyanate contains only three NCS^- anions. This may be a consequence of the following two processes: the disproportionation of

$Y(NCS)_3.6H_2O$ or the formation of the salt $bpyH^+…NCS^-$. The disproportionation (autocomplex formation) of halide complexes into cationic and anionic forms in various solvents is long known.[10] We examined this possibility by the recrystallization of the starting sample of $Y(NCS)_3.6H_2O$ in MeCN and thf. According to the X-ray powder diffraction data, new phases formed in none of the cases. To verify the formation of the salt, we prepared $\{Hbpy\}NCS.1.5H_2O$ and $\{H_2bpy\}(NCS)_2$ [11] and identified them by single-crystal X-ray diffraction. However, we failed to detect these salts in the impurity phases that were formed along with **3**. Most likely, the anions of these salts are incorporated into the coordination sphere of yttrium giving rise to thiocyanate anions of yttrium. This is confirmed by a particular time dependence of this process and the dependence on the bpy concentration, as well as by the fact that bpy molecules are present in the solvation sphere of supramolecular assembly **3**. The absence of **3** in alcoholic solutions and the formation of **3** as the main phase in aprotic solvent (MeCN and thf) are undoubtedly associated with the solvation effects. This is supported by the detection of **3** in i-PrOH, which is intermediate as the solvent between lower aliphatic alcohols (methanol, ethanol) and aprotic solvents (MeCN, thf).[7] A forced increase in the NCS : Y ratio in the solution by the addition of an aqueous solution of HNCS to the alcoholic solution resulted in the formation of **3** in virtually quantitative yield. According to the X-ray powder diffraction data, this product contains **3** as the main phase (~80%). The monomer $\{Hbpy\}[Y(H_2O)_3(NCS)_4]\cdot 2bpy\cdot 2H_2O$ (**4**) was found as an impurity, like in the synthesis in MeCN and thf. Besides, the salt $\{Hbpy\}_4[Y(H_2O)_3(NCS)_5]\cdot(NCS)_2\cdot H_2O$ (**7**) was obtained as another impurity. Assembly **3** is readily soluble in ethanol. This is why a polycrystalline product was obtained, after the slow crystallization, in the synthesis with HNCS. An analysis of the positions of the characteristic absorption bands in the IR spectra of **1 – 3** and their comparison with the data for the starting reagents showed that the most substantial changes are observed for the band ν(NC) of the thiocyanate ligand. The formation of **1 – 3** is accompanied by the low-frequency shift of this band, on the average, by 30 cm^{-1} and it loses the initial structuring. Let us also mention small changes in the position of ν(Y-O); the other shifts are less significant.

X-ray diffraction study

The structure of **1** consists of complex molecules and bpy molecules of solvation (Fig. 1a). Six of the seven hydrogen atoms of the coordinated H_2O and EtOH molecules are involved in O-H…N(S) hydrogen bonding. The structural units are linked to each other by six hydrogen bonds to form two interpenetrating 3D networks. Figure 2a, b displays the structure of an independent network, in which the structural units are related by translations and a 2_1 axis parallel to the crystallographic axis a; the second network is related to the former one by 2_1 axes parallel to the crystallographic axes b and c.

The crystal structure of **2** contains centrosymmetric dimeric molecular complexes (Fig. 1b) and bpy and i-PrOH molecules of solvation. One of such bpy molecules has the crystallographic symmetry -1. The i-PrOH molecule is connected to the complex by two hydrogen bonds, as a donor to a hydrogen atom of coordinated H_2O and as a O-H…S hydrogen bond acceptor to form the associate (μ-bpy)[$Y(NCS)_3(H_2O)_3$]$_2$·2(i-PrOH). The associates are linked by bpy molecules of solvation to form two interpenetrating 3D networks (Fig. 3 a, b). Figure 3b displays the hydrophobic region of the structure formed by aliphatic i-PrOH.

The centrosymmetric dimeric anionic complexes (Fig. 1c) in structure **3** and the monoprotonated cations Hbpy are linked by N-H…N hydrogen bonds (the coordinated nitrogen atoms of the NCS ligand act as acceptors). In addition, the structure contains bpy molecules of solvation. The acidic hydrogen in Hbpy was located in a difference Fourier map. The structural units are held together by N-H…N and O-H…N(S) hydrogen bonds to form two interpenetrating 3D networks (Fig. 4, S1).

The crystal structure of **4** is composed of anionic complexes, monoprotonated Hbpy cations (Fig. 1d), bpy molecules of solvation, and water molecules of crystallization. The N(6)…N(8) distance (2.695 Å) is indicative of the formation of a N-H…N hydrogen bond. The difference Fourier map shows two peaks of approximately equal height in the vicinity of the N(6) (at a distance of 1.19 Å) and N(8) (at a distance of 1.10 Å) atoms. In the structure refinement, these peaks were interpreted as hydrogen atoms with 0.5 occupancies. Each of the three coordinated water molecules is "continued" as $H_x$bpy (x = 0, 1). The complex anions and water molecules of crystallization are linked together to form layers perpendicular to the c axis, and the layers are linked by $H_x$bpy to form 3D networks.

The composition of compound **5** can formally be written as {Hbpy}$_3$[$Y(H_2O)(NCS)_6$].bpy. However, the difference Fourier map shows four peaks in the vicinity of the nitrogen atoms of four independent bpy ligands. Hence, we suggest the formula {H_3(bpy)$_4$}[$Y(H_2O)(NCS)_6$]. Two peaks, like those in structure **4**, correspond to one disordered hydrogen atom (N…N, 2.655 Å), and we assigned occupancies 0.33 and 0.67 to these sites based on the heights of the peaks. The coordinates and displacement parameters of all hydrogen atoms (except for disordered hydrogens) in structure **5** were refined independently. For the disordered atoms, only displacement parameters were refined. Seven of the eight nitrogen atoms of Hbpy are involved in hydrogen bonding as hydrogen donors and acceptors. Two disordered hydrogen atoms form an associate {bpy-H…bpy}, which is connected to the anionic complex by a O-H…N hydrogen bond, and the centrosymmetric moiety ({bpy-H…bpy}[$Y(H_2O)(NCS)_6$])$_2$ in structure **5** is formed through O-H…S hydrogen bonds (Fig. 1e). The associates {bpy-H…bpy} are linked by N-H…N and C-H…N hydrogen bonds to zigzag 1D chains (Fig. 5), which,

together with the complex anions, form 2D networks perpendicular to the x axis. Two Hbpy cations, which are not involved in this network, are linked by N-H…N hydrogen bonds giving rise to two independent chains parallel to the z axis.

The crystal structure of **6** is composed of polymer chains parallel to the [1 0 -1] direction (Fig. 1f) and Hbpy cations. The quality of the crystal (plates with a thickness of 0.01 mm) allowed us to locate only one of the six hydrogen atoms active in hydrogen bonding. The structural units are linked through N-H…N and O-H…N(S) hydrogen bonds to form three interpenetrating 3D networks.

The crystal structure **7** contains two crystallographically independent structurally identical discrete anionic complexes (Fig. 1g), four independent NCS^- anions, four water molecules of crystallization, and eight H_xbpy groups. Since eight protons are required for the charge compensation, it would be suggested that the structure contains eight monoprotonated $Hbpy^+$ ions. However, the degree of their protonation can be unambiguously determined only for two nitrogen atoms (one atom is an O-H…N hydrogen bond acceptor, and another is an N-H…S hydrogen bond donor). The other 14 nitrogen atoms are involved in N-H…N hydrogen bonding (two nitrogen atoms per hydrogen bond), and the formation of H_2bpy^{2+} + bpy pairs is theoretically possible. The crystal structure of **7** is such that the degree of protonation of particular H_xbpy is of no importance for the packing of the structural units. Hence, we will designate these ligands as Hbpy. The complexes, NCS^- anions, and water molecules of crystallization form 2D networks parallel to the (1 0 1) plane, which are linked through {Hbpy…Hbpy} dimers to form 3D networks (Fig. 7a). The remaining six Hbpy molecules are involved in two crystallographically independent 1D chains $\{Hbpy\}_n$ (both chains are parallel to the [1 0 1] direction) with three independent cations held together by stacking interactions per chain (Fig. 7b). These doubled chains pass through 3D networks.

In the seven structurally characterized compounds, the Y : bpy ratio is 1 : 2 (**1**-**3**), 1 : 3 (**4**, **6**), or 1 : 4 (**5**, **7**). Despite different compositions and arrangement of the structural units, compounds **1**-**3** have similar crystal structures. Thus, all structures have a primitive rectangular 2D network perpendicular to one of the crystallographic directions (in all cases, to the a axis) (Figs. 2a-4a), the nodes of which are occupied by Y complexes, and the edges are formed by bpy (monocoordinated, bridging, protonated groups, or molecules of solvation). The network metrics is 14.09 x 15.67, 13.96 x 15.37, and 14.10 x 15.46 Å in **1**-**3**, respectively (b, c for **1**; b, c*sin(β) for **2** and **3**), The 2D networks are linked by O-H…S hydrogen bonds to 3D networks (the distance between the 2D networks corresponds to one-half of the unit cell parameter a). The 3D network contains large cavities occupied by another, identical, interpenetrating network. Since in all three structures under consideration, two independent networks are related by a 2_1 axis, the

complexes belonging to one network occupy the centers of the cavities of the second network, and the planar bpy molecules intersect each other (Fig. 3c exemplifies the whole unit cell of compound **3**) An increase in the number of bpy groups in the structure leads to a greater ambiguity in the crystal packing, the structure of which is determined mainly by the anionic complex (Fig. 1d-g). It should be noted that the aggregation of bpy was found in all compounds **4**-**7**. Thus, compound **4** contains bpy…Hbpy dimers, zigzag 1D chains are present in structure **5** (Fig. 5), and linear 1D chains are present in **6** and **7** (Fig. 7b). The bond lengths and bond angles in structures **1** – **7** are typical of such compounds. The CN of yttrium in compounds **1**, **3**, **6**, and **7** is 8; in assemblies **2**, **4**, and **5**, Y^{3+} has CN 7.

Thermal behavior

The low-temperature behavior of the complexes is considered using the starting complex $[Y(H_2O)_5(NCS)_3]\cdot H_2O$ and the synthesized compound $[Y(H_2O)_3EtOH(bpy)(NCS)_3]\cdot bpy$ (**1**) as examples. The experimental data obtained by adiabatic calorimetry were smoothed using known approaches.[12] The experimental adiabatic calorimetry data were also used to calculate the thermodynamic functions of the compounds (Table S1.). The low-temperature heat capacity of yttrium triisothiocyanate hydrate $Y(NCS)_3(H_2O)_6$ was measured in the study. [13] Table 1 compares our data and the results published in the study;[13] a slight discrepancy in the results (the difference in the standard entropy is 1%) may be attributed, first, to the difference in the temperature range under investigation (we carried out the measurements starting from 6 K, whereas the measurements in the study[13] were performed from 13 K) and, second, to the difference in the procedure used for the extrapolation to 0 K.

Table 1. Comparison of standard thermodynamic functions of yttrium thiocyanate

Characteristics	$[Y(H_2O)_5(NCS)_3]\cdot H_2O$	$Y(NCS)_3(H_2O)_6$ [13]
$C_p^0(298.15)$, J/(K mol)	447.7	454.2
$S^0(298.15)$, J/(K mol)	516.6	511.6
$H^0(298.15)-H^0(0)$, J/mol	76250	77240

Figure 8 displays the temperature dependence of the heat capacity calculated from the experimental adiabatic calorimetry data. It can be seen (Fig. 8) that no anomalies were found in the $C_p^0(T)$ dependence for $[Y(H_2O)_5(NCS)_3]\cdot H_2O$, the molecular and crystal structure of which was determined earlier,[6] in the range from helium temperatures to 76 ºC, whereas an anomaly with T_{max}= 241.3 K and ΔS^0 = 0.45 J/(K mol) is observed for the assembly $[Y(H_2O)_3EtOH(bpy)(NCS)_3]\cdot bpy$ (**1**) in the range of 225 – 250 K (from -48 to -23 ºC). No

substantial structural differences for this assembly above and below the temperature of this anomaly were found. Hence, this anomaly is apparently associated with certain thermal variations in the architecture of assembly **1**.

The thermal analysis showed that, like the starting complex $[Y(H_2O)_5(NCS)_3].H_2O$,[6] complex **1** is stable up to 76±1 ºC (Fig. 9 and S2.). At higher temperatures, the thermal decomposition starts. In the temperature range of 76 - 140 ºC, the weight loss is Δm = 13.5±1.0%. According to the DTA and DSC data, this is a one-step process accompanied by heat release. The gas-phase mass spectrum showed the ions $[H_2O]^+$, $[OH]^+$, $[C_2H_6O]^+$, $[C_2H_5O]^+$, $[C_2H_3O]^+$, $[CH_3O]^+$, $[CH_2O]^+$, and $[CH_3]^+$. These results provide evidence that the first step corresponds to the removal of the coordinated water and ethanol molecules (the content of H_2O and EtOH calculated from the empirical formula is 14.8%). The resulting intermediate remains intact without changes in the composition up to 210 ºC. At higher temperatures, a rather intricate multistep process takes place (210 - 440 ºC, ∑Δm = 66.8±1.5%). The gas-phase mass spectrum showed the ions $[C_{10}H_8N_2]^+$, $[C_{10}H_7N_2]^+$, $[C_8H_6N_2]^+$, $[C_8H_5N_2]^+$, $[C_9H_8]^+$, $[C_8H_7]^+$, $[C_5H_4N]^+$, $[C_4H_3]^+$, $[CHN]^+$, $[CN]^+$, and $[CH_3]^+$. According to the DSC, DTA, and the analysis of gases evolved during a TGA experiment, at least the two-step decomposition is clearly seen. The first step of this intricate process involves the releases of bpy molecules of solvation (t_{fus} = 114 ºC, t_{boil} = 305 ºC), the evaporation of which becomes noticeable at 210 ºC. The major portion of bpy is transferred into the gas phase, and the remainder boils at 305 ºC (a small endothermic peak). At temperatures above 314 ºC, coordinated bpy is apparently detached and completely removed from the intermediate, which is accompanied by the decomposition of NCS^- (the mass spectrum shows the ion $[CN]^+$). The total weight loss in the temperature range under study is ∑ Δm = 81.2%. The study of the thermal behavior of assembly **2** revealed a somewhat different pattern (the boiling point of i-PrOH is 82 ºC) (Fig. 9). In the temperature range of 50 – 160 ºC, the weight loss is 17±1.0%, two peaks are observed in the DTA/DSC curve, and the main peaks in the mass spectrum are assigned to $[H_2O]^+$ and $[C_3H_9]^+$. In the first step, the coordinated water and i-PrOH molecules are removed (the content of H_2O and i-PrOH calculated from the empirical formula is 16.5%). In the temperature range of 160- 230 ºC, the weight loss takes place (Δm = 33.5±1.0%, which corresponds to the content of bpy molecules of solvation calculated from the empirical formula) accompanied by a considerable endothermic effect. The analysis of gases evolved during a TGA experiment showed ions corresponding to the electron-impact-induced fragmentation of 4,4'-bipyridine. The low, compared to compound **1**, temperature of the onset of the removal of bpy is attributed to the structural features of the assembly. At temperatures above 230 ºC, the thermal destruction is virtually identical to the decomposition of compound **1**, which involves the two-step removal of the remaining bpy molecules and the

decomposition of NCS^-. The character of decomposition of anionic dimeric assembly **3** is rather similar to that of compound **1**. The onset of the weight loss (DTA curve) is observed at temperatures above 85 ºC; in the range of 85 - 170 ºC, the coordinated water molecules are released step-by-step (DSC and DTA curves) ($\Delta m = 8.6\pm1.0\%$, which corresponds to the 7.8% content of coordinated water molecules calculated from the empirical formula). As in the case of compound **1**, the formation of an intermediate was observed. However, the temperature range, in which this intermediate remains intact without changes in the composition, is more narrow (180 - 230 ºC). A rather intricate multistep process starts at temperatures above 230 ºC (230 - 480 ºC, $\sum\Delta m = 66.8\pm1.5\%$). The gas-phase mass spectrum is represented mainly by ions corresponding to the electron-impact-induced fragmentation of 4,4'-bipyridine.

Fluorescence

Earlier, we have measured the excitation and emission spectra for KSCN and the complex $[Y(H_2O)_5(NCS)_3]\cdot H_2O$.[7] The emission bands in the spectra were broad and virtually unstructured. This suggests that the fluorescence of the SCN^- ions plays a key role in the properties of the complex $[Y(H_2O)_5(NCS)_3]\cdot H_2O$. We studied the fluorescence of the following complexes in the solid state at room temperature: the molecular assemblies $[Y(H_2O)_3EtOH(bpy)(NCS)_3)]\cdot bpy$ (**1**), $\{(\mu\text{-bpy})[Y(H_2O)_3(NCS)_3]_2\}\cdot 3bpy\cdot 2(i\text{-PrOH})$ (**2**), and the assembly $[Hbpy]_2\{(\mu\text{-bpy})[Y(H_2O)_3(NCS)_4]_2\}\cdot bpy$ (**3**) composed of the anionic complex and the monoprotonated cation Hbpy. The excitation spectra (Fig. 10) were detected at 450 nm. They consist of two bands with maxima at 234 and 258 nm. But in contrast to the excitation spectrum of $[Y(H_2O)_5(NCS)_3]\cdot H_2O$ (black curve, Fig. 10), the bands in spectra of **1-3** are distinct. This is evidence of the involvement of the 4,4'-bipyridine ligand in the energy transfer. The bands in the emission spectra measured using excitation at a wavelength of 238 nm are broad, asymmetric, and almost unstructured. Each emission spectrum can be satisfactorily described by two polynomials with maxima at 445 and 465 nm, respectively. It can be seen from fig. 10 that maximum of the emission band in $[Y(H_2O)_5(NCS)_3]\cdot H_2O$ spectrum is approximately 430 nm. Thus we can conclude that the presence of an additional organic ligand apparently leads to a long-wavelength shift of the emission maximum.

Conclusions

Although the procedure used for the synthesis of assemblies **1 – 3** is rather simple, the rate of crystallization, the phase homogeneity, and the yield are very sensitive to the nature of the solvent system, which not only determines the composition of molecular assemblies (ethanol, i-

PrOH) but also influences the formation of supramolecular aggregates based on anionic complexes of yttrium (i-PrOH, MeCN, thf). In ethanol, assembly **1** forms as a result of the self-assembly, which is not accompanied by the generation of impurities. In aprotic solvents, and partly in i-PrOH, the formation of **3** depends on ditopic 4,4'-bpy, in the presence of which the redistribution of the NCS^- ligand takes place to give **3** – **6** containing a larger number of anionic ligands in the coordination sphere. This is indicative of the formation of complexes with a higher degree of aquation of the coordination sphere of yttrium and is supported by the yield of **3** (~50%). We observed a similar situation for ditopic phenanthroline. Thus, the reaction of $[Y(H_2O)_5(NCS)_3]\cdot H_2O$ with 4,7-phen gave $[Y(H_2O)_7(NCS)](NCS)_2\cdot 5(4,7\text{-phen}).5(H_2O)$.[14] The supramolecular aggregation in **1** – **3** occurs through various hydrogen bonds. The similar packing mode of **1** and **3** is reflected in the similarity of the thermal decomposition of these compounds. The effect of 4,4'-bpy on the fluorescence of yttrium thiocyanate found in the present study holds promise for designing new nitrogen-containing ligands, which can increase the luminescence intensity of thiocyanate complexes.

Experimental

General

The commercial reagents $[Y(H_2O)_5(NCS)_3].H_2O$,[6] bpy (Aldrich) and the solvents MeOH, EtOH, *i*-PrOH, thf, MeCN, Et_2O were used as is without additional drying or purification. All reactions were carried out in air at room temperature. An aqueous solution of HNCS was prepared by the reaction of a solution of $Ba(NCS)_2.3H_2O$ (Vecton, reagent grade) with an equimolar amount of a sulfuric acid standard solution (FIXANAL).

The elemental analysis was performed according to standard procedures on an EA1108 Carlo Erba CHN analyzer in the Center for Collaborative Research of the Kurnakov Institute of General and Inorganic Chemistry of the Russian Academy of Sciences (IGIC RAS). The IR spectra were recorded in the Center for Collaborative Research of IGIC RAS on a Nicolet Nexus FTIR spectrometer in the region of 550 – 4000 cm^{-1}. The X-ray powder diffraction study was performed on a STOE STADI P diffractometer ($CuK_{\alpha 1}$ radiation, Ge monochromator) in the Center for Collaborative Research of the Lomonosov Moscow State University.

The heat capacity of **1** and $[Y(H_2O)_5(NCS)_3]\cdot H_2O$ was measured in the temperature range of 5-298 K in an automatic mode on a BKT-3 low-temperature adiabatic calorimetric setup designed and manufactured by the TERMIS LLC. Weighed samples (0.26396 and 0.5549 g, respectively), were placed in a thin-walled titanium cylindrical container with an inner volume of

1 cm^3. The container was sealed in a special chamber under a helium atmosphere at a pressure of ≈0.3 bar. The temperature of the calorimeter was measured with a rhodium-iron resistance thermometer. The sensitivity of the temperature-measuring system was 10^{-3} K; the sensitivity of the analog-to-digital converter was 0.1 μV. The energy equivalent of the calorimeter was determined by measuring the heat capacity of the empty tube filled with gaseous helium under a pressure of 8.5 kPa. The accuracy of the heat capacity measurements at helium temperatures is ±2%, decreases to ±0.4% as the temperature increases to 40 K, and is ±0.2% in the range of 40–350 K. [15]

The thermal behavior of the compounds was studied by differential scanning calorimetry (DSC) and thermogravimetry (TG) on *NETZSCH DSC 204 F1* and *NETZSCH TG 209 F1* instruments, respectively.[7] Photoluminescence was measured on an LS5 spectrometer (Perkin Elmer) in the region of 200 - 700 nm at room temperature; the resolution was 0.5 nm; the slit width was varied from 4 to 10 nm. The attachment for measurements of solid-state luminescence was used.

Synthesis

$[Y(H_2O)_3EtOH(bpy)(NCS)_3]\cdot bpy$ (1). A solution of yttrium thiocyanate (0.36 g, 0.96 mmol) in ethanol (10 mL) was added with stirring to a solution of bpy (0.31 g, 1.96 mmol) in ethanol (15 mL). The isothermal evaporation of the homogeneous solution for two weeks afforded pinkish crystals, which were separated on a glass filter, washed with ethanol, and dried in a vacuum desiccator over silica gel. The yield was 0.3 g, 46% based on Y. ATR-IR, ν/cm^{-1} : 3384 ν(H_2O), 2063 ν(NC), 1650 δ(H_2O), 1595 ν(CN), 1406 ν(C-C), 807 δ(CH), 621, 575 ν(Y-O). X-ray powder diffraction, pure product **1**. Found: C, 44.8; H, 3.6; N 13.8; S 16.0. $C_{25}H_{28}N_7O_4S_3Y$ requires C, 44.4; H, 4.1; N, 14.5; S 14.2%; M, 675.6.

$\{(\mu\text{-bpy})[Y(H_2O)_3(NCS)_3]_2\}\cdot 3bpy\cdot 2(i\text{-}PrOH)$ (2).

A. Yttrium thiocyanate (0.28 g, 0.76 mmol) was dissolved in EtOH (10 mL). The solution was filtered into a solution of bpy in EtOH (15 mL; bpy : Y = 3.96), and a homogeneous solution was obtained. A solid phase formed in 3 days. According to the X-ray powder diffraction data, **1** was obtained as the main phase (>90%)**.** The solid phase was mixed with i-PrOH, and the heterogeneous solution was *immediately* evacuated on a glass filter. Crystals of **2** were identified from the thus prepared product and from the crystals that were present in the mother liquor. ATR-IR, ν/cm^{-1} : 3389 ν(H_2O), 2065 ν(NC), 1635 δ(H_2O), 1595 ν(CN), 1406 ν(C-C), 799 δ(CH), 620 ν(Y-O). Found: C, 47.8; H 4.1; N 14.8; S 11.9. $C_{52}H_{60}N_{14}O_8S_6Y_2$ requires C, 45.3; H 4.3; N 14.2; S 12.9%; M, 1379.

B. A cream solution of yttrium thiocyanate (0.43 g, 1.17 mmol) in i-PrOH (20 mL) was filtered into a colorless solution of bpy (0.33 g, 2.12 mmol) in i-PrOH (20 mL), resulting in the formation of a homogeneous solution. The isothermal evaporation of the solution for three weeks afforded a solid phase. Then i-PrOH was added for the partial dissolution. After four days, the crystals were separated on a glass filter, washed with i-PrOH, and dried in a vacuum desiccator over silica gel. The yield was 0.12 g, 15% based on Y. ATR-IR, ν/cm^{-1}: 3389 ν(H_2O), 2065 ν(NC), 1635 δ(H_2O), 1598 ν(CN), 1406 ν(C-C), 800 δ(CH), 620 ν(Y-O). Found: C, 43.9; H, 3.8; N, 14.3; S, 12.4. $C_{52}H_{60}N_{14}O_8S_6Y_2$ requires C, 45.2; H, 4.4; N, 14.2; S, 12.8%; M, 1379. Crystals of **2** and **3** were found in the mother liquor.

$[Hbpy]_2\{(\mu\text{-bpy})[Y(H_2O)_3(NCS)_4]_2\}\cdot bpy$ (**3**). A solution of yttrium thiocyanate (0.36 g, 0.98 mmol) in MeCN (15 mL) was added to a solution of bpy (0.29 g, 1.86 mmol) in MeCN (20 mL), after which the solid phase immediately precipitated. The separation was performed on a paper filter followed by drying in a vacuum desiccator over silica gel. The yield was0.36 g, 54 % based on Y. ATR-IR, ν/cm^{-1}: 3382 ν(H_2O), 2092, 2062 ν(NC), 1635 δ(H_2O), 1598 ν(CN), 1406 ν(C-C), 818 δ(CH), 621 ν(Y-O). Found: C, 41.0; H, 3.9; N, 14.5; S, 18.6. $C_{48}H_{46}N_{16}O_6S_8Y_2$ requires C, 41.8; H, 3.4; N, 16.2; S 18.6%; M, 1377.

Synthesis of 3 in the presence of HCNS. A weighed sample of $Y(NCS)_3.6H_2O$ (0.34 g, 0.93 mmol) was dissolved in ethanol (15 mL), an aqueous solution (2.5 mL) of HNCS (1 mmol) was added, and this solution was poured into a solution of bpy (0.298 g, 1.91 mmol) in ethanol (25 mL). The homogeneous pink solution was concentrated in air, under conditions of isothermal evaporation, to obtain beige crystals. All crystals were poured with CH_3CN, transferred to a glass filter, and washed with MeCN. The yield was 0.57 g, 89% based on Y. Found: C, 44.2; H, 3.6; N, 16.6; S, 17.2. $C_{48}H_{46}N_{16}O_6S_8Y_2$ requires C, 41.8; H, 3.4; N, 16.2; S 18.6%; M, 1377.

X-ray data collection

X-ray diffraction data were collected on a Bruker SMART APEX2 diffractometer[16] (Table S2.) in the Center for Collaborative Research of IGIC RAS. All three examined crystals of compound **2** were weakly diffracting pseudomerohedral twins. Semiempirical absorption corrections from equivalents were applied using SADABS[17a] for **1**, **3** - **7** and TWINABS[17b] for **2**. All structures were solved by direct methods combined with Fourier map calculations. The lack of an inversion center in structures **1** and **7** was confirmed using the PLATON software.[18] The crystal of **1** is a racemic twin with a 0.312 : 0.688(9) domain ratio. In the crystal structure of **4**, the oxygen atom of one hydrate water molecule is disordered over two positions with a 0.60 : 0.40 occupancy ratio. The occupancies of the disordered positions were refined isotropically with fixed atomic displacement parameters and were then kept fixed in subsequent calculations. All pyridine

moieties of bpy in structure **7** were refined using the SAME instruction. Some hydrogen atoms were located in difference Fourier maps and the other were positioned geometrically. All calculations were carried out using the SHELXS-2013 and SHELXL-2013 software.[19]

Poor quality of impurity phase single crystals **6** ($2\theta_{max}$ 45°, R_{int} 0.13, R_σ 0.12) and **7** ($2\theta_{max}$ 40°, R_{int} 0.13, R_σ 0.39) resulted low precision structure determination; however, there is no doubt in the correctness of the molecular and crystal models of these structures.

Acknowledgments

This study was supported by the Russian Foundation for Basic Research (project nos. 14-03-00470 and 13-03-12428), the Council on Grants of the President of the Russian Federation (Program for State Support of Leading Scientific Schools, grant NSh-1712.2014.3), the Presidium of the Russian Academy of Sciences, and the Department of Chemistry and Materials Science of the Russian Academy of Sciences.

Notes and references

1. J.-M. Lehn: *Supramolecular Chemistry – Concepts and Perspectives*, Wiley-VCH, Weinheim 1995.
2. A.B. Ilyukhin and S.P. Petrosyants, *Rus. J. Inorg. Chem*., 2012, **57,** 1653.
3. J.C. Muñoz, A. M. Atria, R. Baggio, M. T. Garland, O. Peña and C. Orrego, *Inorg. Chim. Acta*, 2005, **358,** 4027.
4. Y. Huang, B. Yan and M. Shao, *J. Solid State Chem*., 2009, **182,** 657.
5. C-Y. Zhang, J-D. Fu and Y-H. Wen, *Acta Crystallogr. Sec. E.,* 2010, **66,** m1519.
6. A. Ilyukhin, Zh. Dobrokhotova, S. Petrosyants and V. Novotortsev, *Polyhedron*, 2011, **30,** 2654.
7. S. Petrosyants, Zh. Dobrokhotova, A. Ilyukhin and V. Novotortsev, *Inorg. Chim. Acta*, 2013, **408,** 39.
8. S. Das, K. Bhar, S. Chattopadhyay, P. Mitra, V. J. Smith, L. J. Barbour and B. K. Ghosh, *Polyhedron*, 2012, **38,** 26.
9. Xiao-Juan Yang, Xiaoqing Liu, Yanyan Liu, Yongjing Hao and Biao Wu, *Polyhedron* 2010, **29**, 934.
10. (a) V. Gutmann, Coordination Chemistry in Non-Aqueous Solutions. Springer-Verlag, Wien, New York, 1968; (b) M. Dalibart, J. Deroualt, P. Granger and S. Chapelle, *Inorg.*

Chem., 1982, **21,** 1040; (c) M.J. Taylor, Polyhedron, 1990, **9,** 207; (d) S.P.Petrosyants and A.B. Ilyukhin, *Rus. J. Coord. Chem*., 2010, **36,** 97.

11. (a) A. B. Ilyukhin and S.P. Petrosyants, *Private Commun.*, 2012, CCDC 901637. (b) A.B. Ilyukhin and S.P. Petrosyants, *Private Commun.*, 2012, CCDC 904879.
12. (a) V.M. Gurevich, O.L. Kuskov, K.S. Gavrichev and A.V. Tyurin, *Geochem. Int*., 2007, **45**, 206; (b) S.W. Kieffer, *Rev. Geophys. Space Phys*., 1979, **17**, 35.
13. Tan Zhicheng, Matsuo Takasuke, Suga Hiroshi, Zhang Zhiying, Yin Jingzhi, Jiang Bengao and Sun Tongshan, *Science in China (Ser. B),* 1997, **40**, 165.
14. S.P. Petrosyants and A.B. Ilyukhin, *Rus. J. Coord. Chem*., 2014, **40**, 401.
15. K.S. Gavrichev, N.N. Smirnova, V.M. Gurevich, V.P. Danilov, A.V. Tyurin, M.A. Ryumin and L.N. Komissarova, *Thermochim. Acta*, 2006, **448**, 63.
16. Bruker (2007). APEX2 and SAINT. Bruker AXS Inc., Madison, Wisconsin, USA.
17 (a) G.M. Sheldrick, SADABS. University of Göttingen, Germany, 1997; (b) G.M. Sheldrick, TWINABS. University of Göttingen, Germany, 1997.
18. Spek, A. L. *J. Appl. Cryst*., 2003, **36**, 73.
19. Sheldrick, G. M. *Acta Crystallogr., Sect. A*, 2008, **64**, 112.

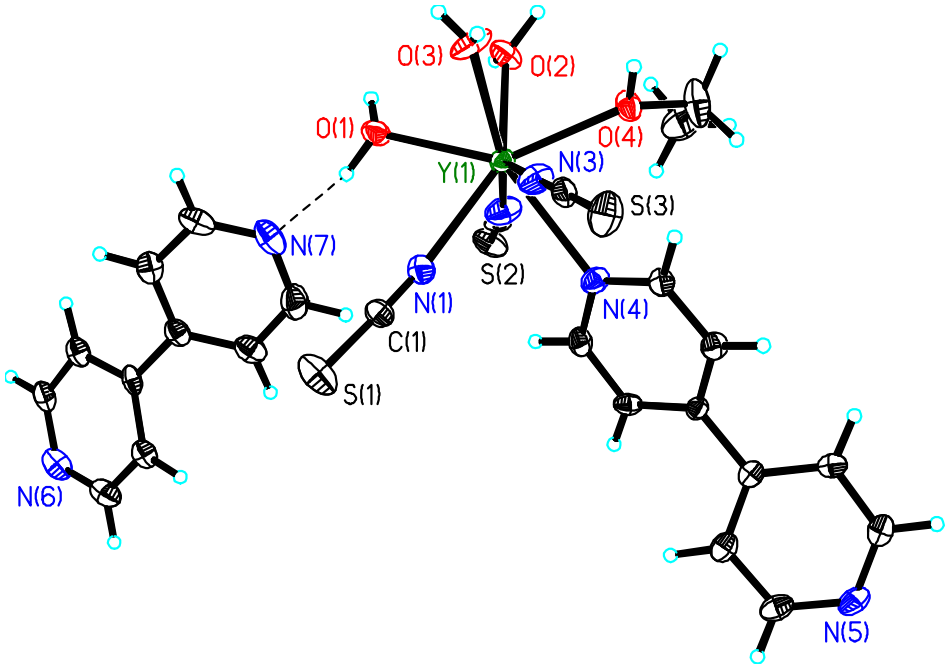

a

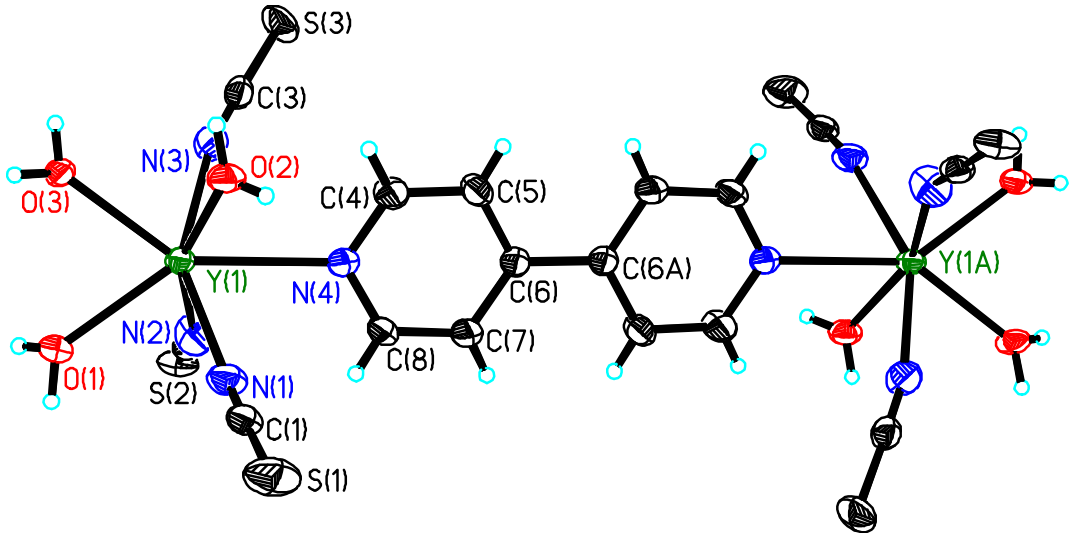

b

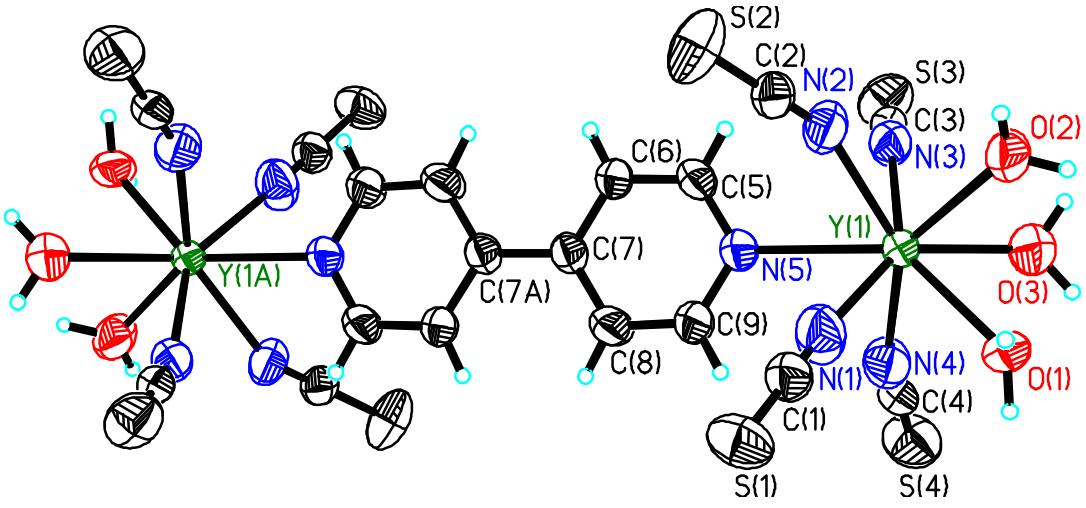

c

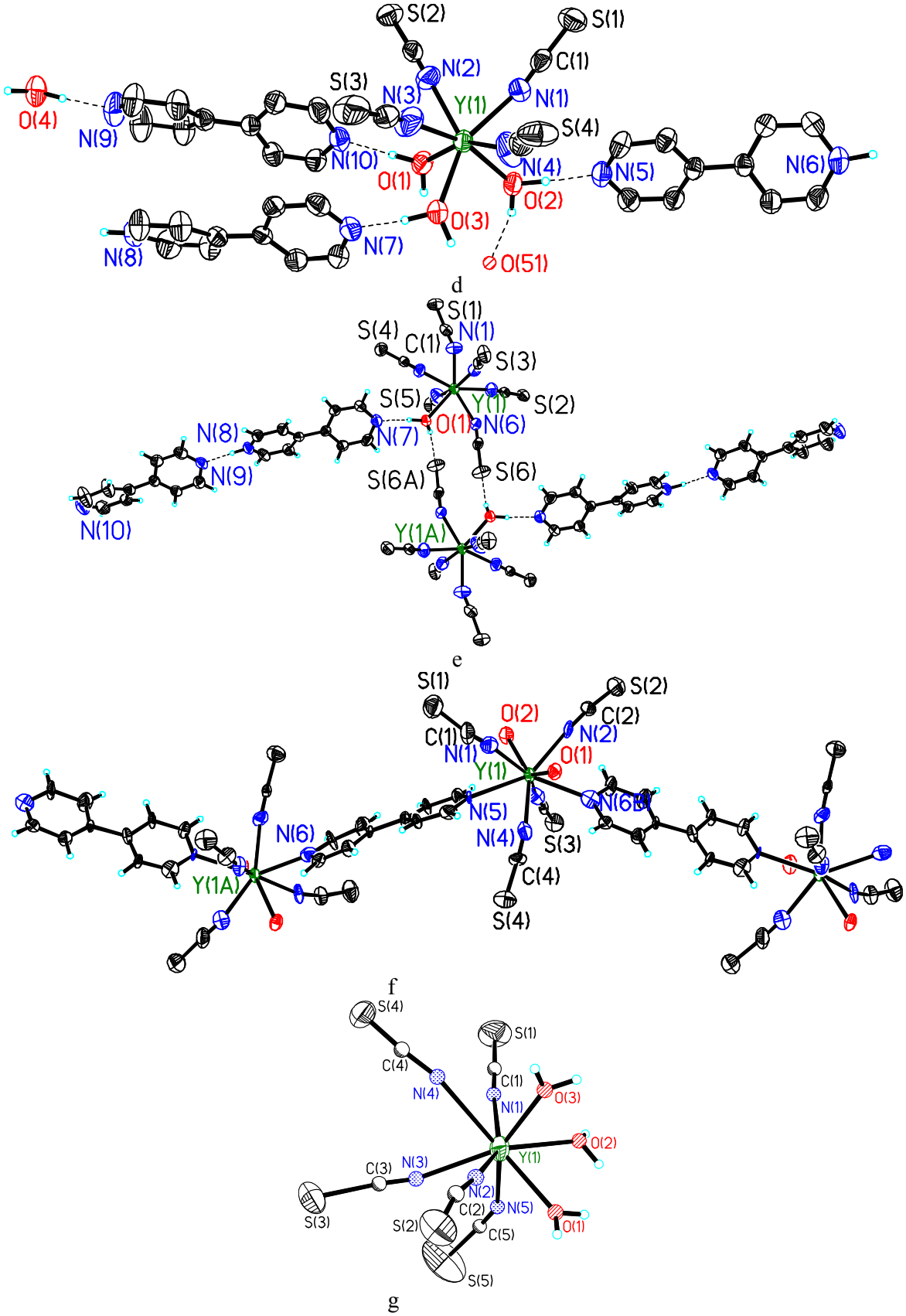

Fig.1. Fragments of structures **1** (a), **2** (b), **3** (c), **4** (d), **5** (e), **6** (f), and **7** (g) (50% probability ellipsoids).

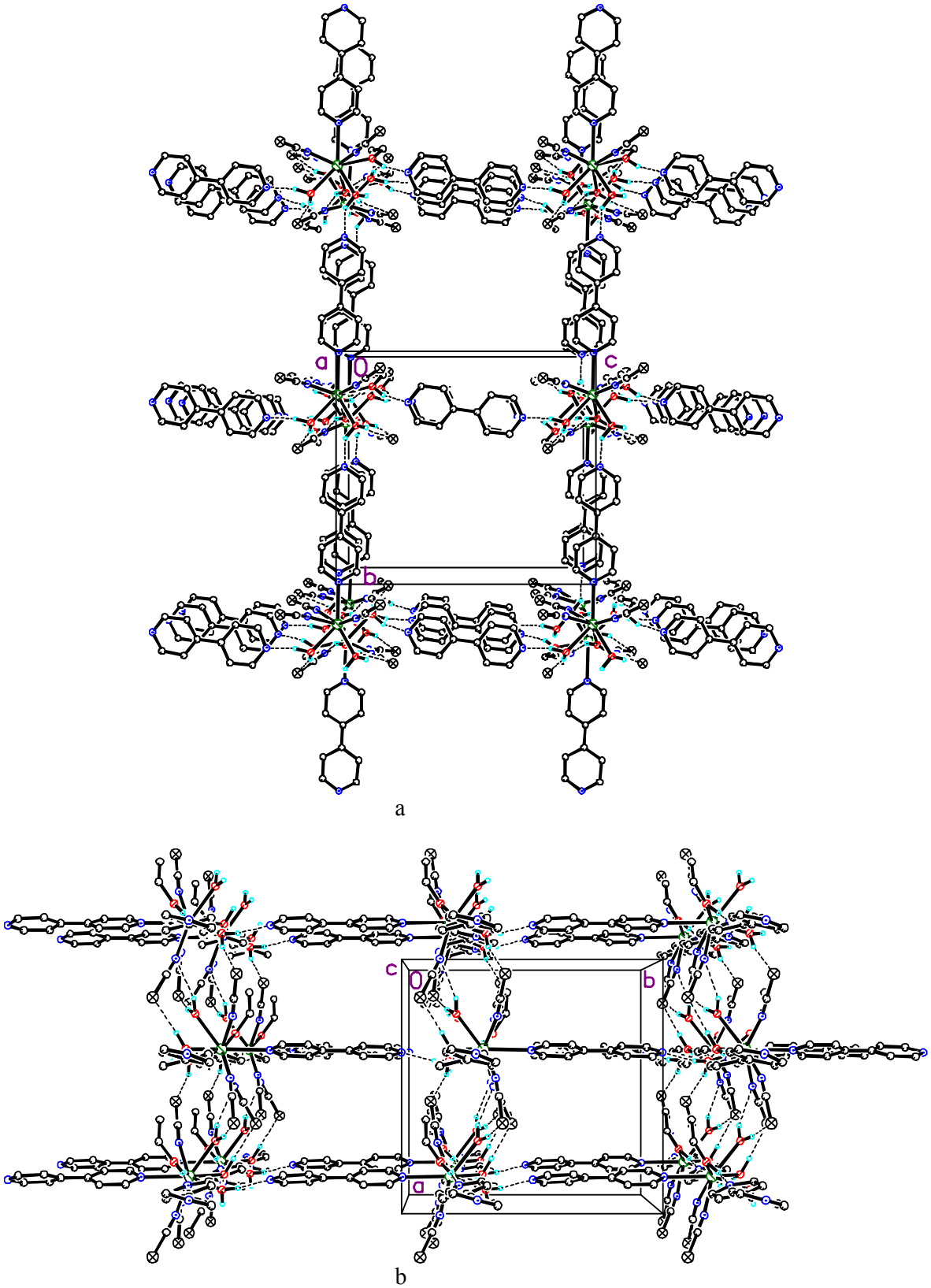

Fig.2. Fragment of structure **1** projected along the a (**a**) and c **(b)** axes**.**

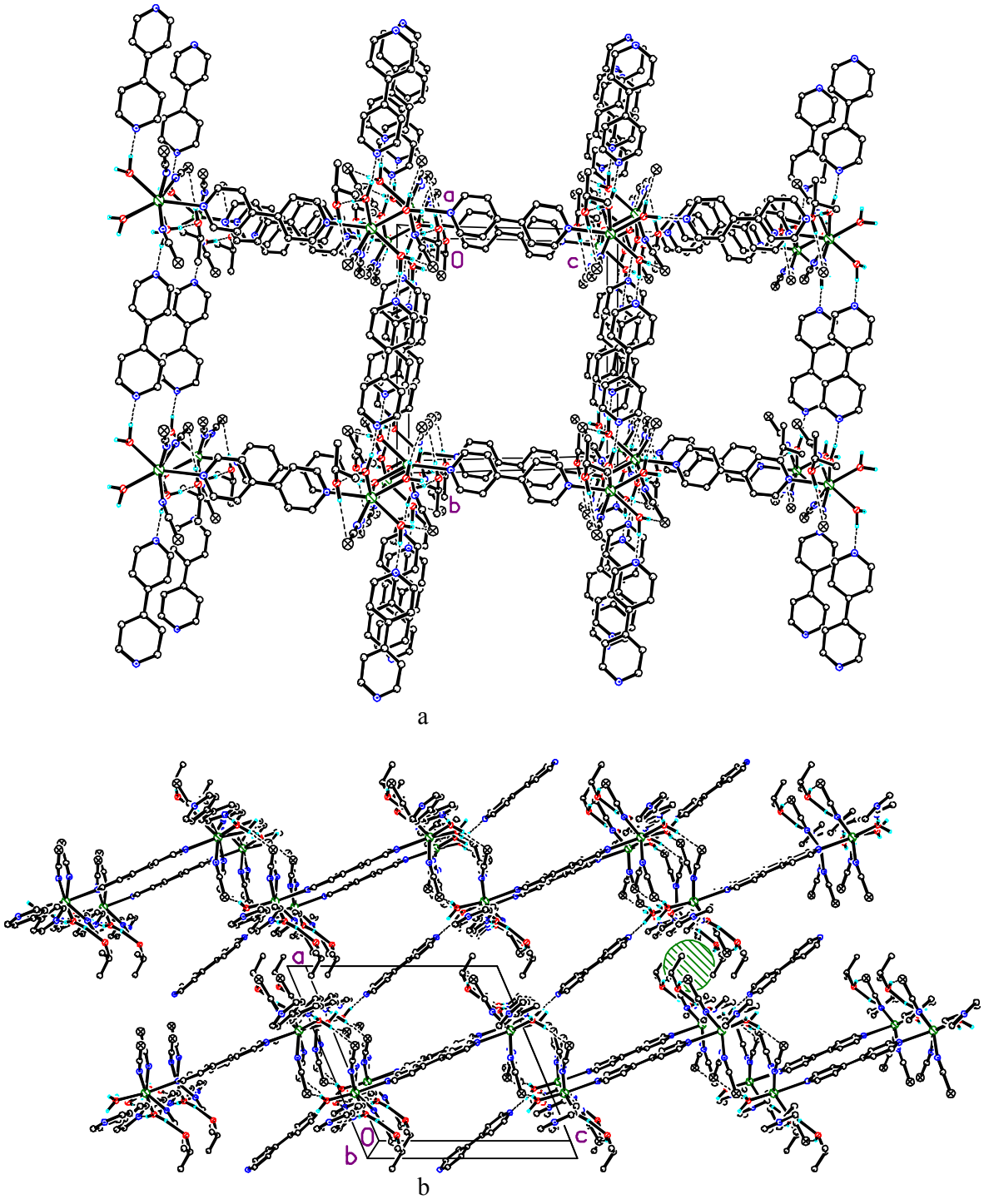

Fig.3. Fragment of structure **2** projected along the a (**a**) and b **(b)** axes**.**

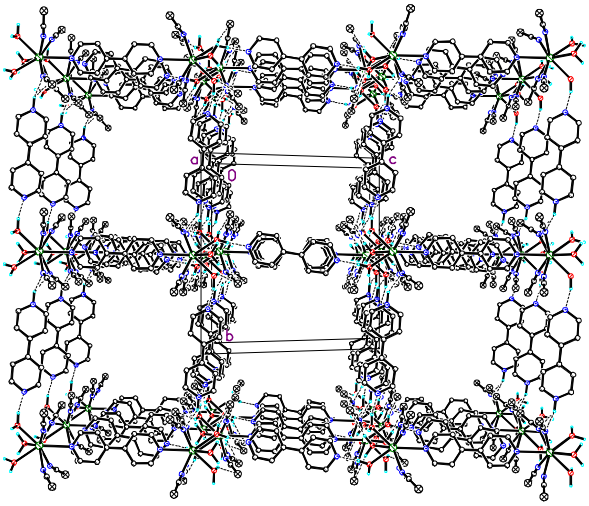

a

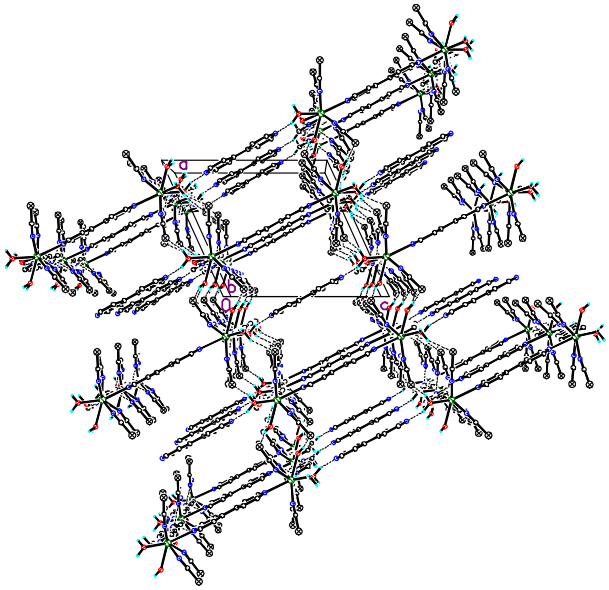

b

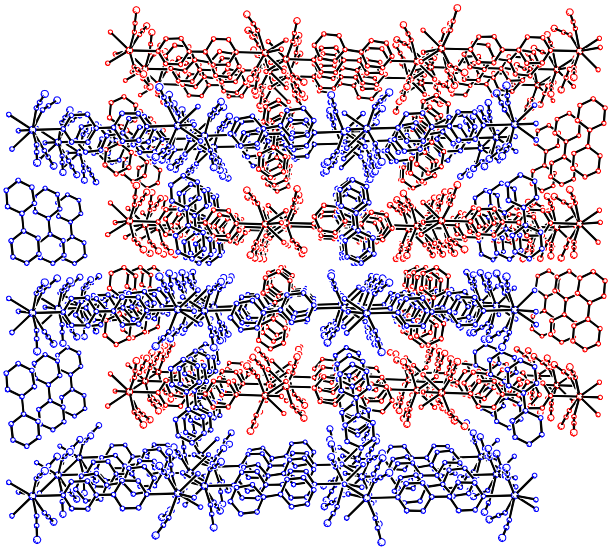

c

Fig.4. Fragment of structure **3** projected along the a (**a**) and b **(b)** axes; the projection of structure **3** along the a axis (c).

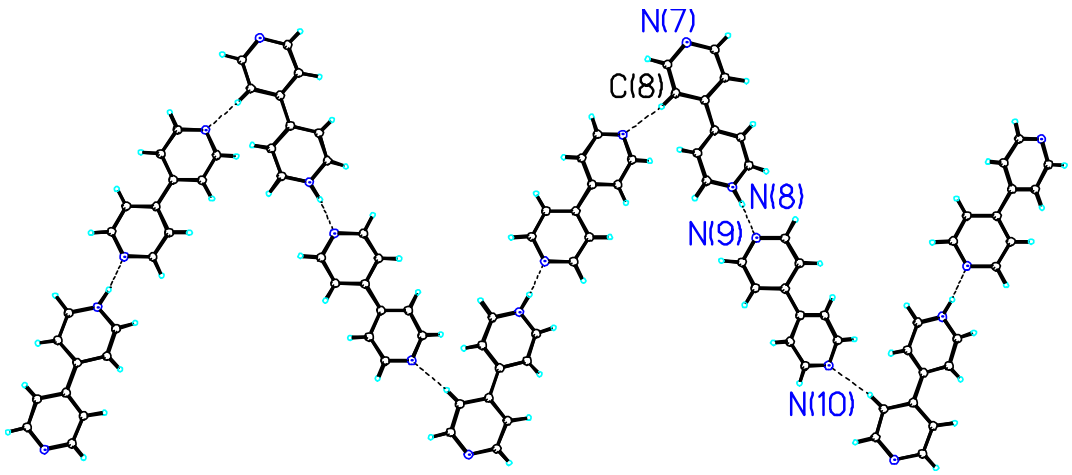

Fig.5. Chains in structure **5**; one position of the disordered hydrogen atoms is shown.

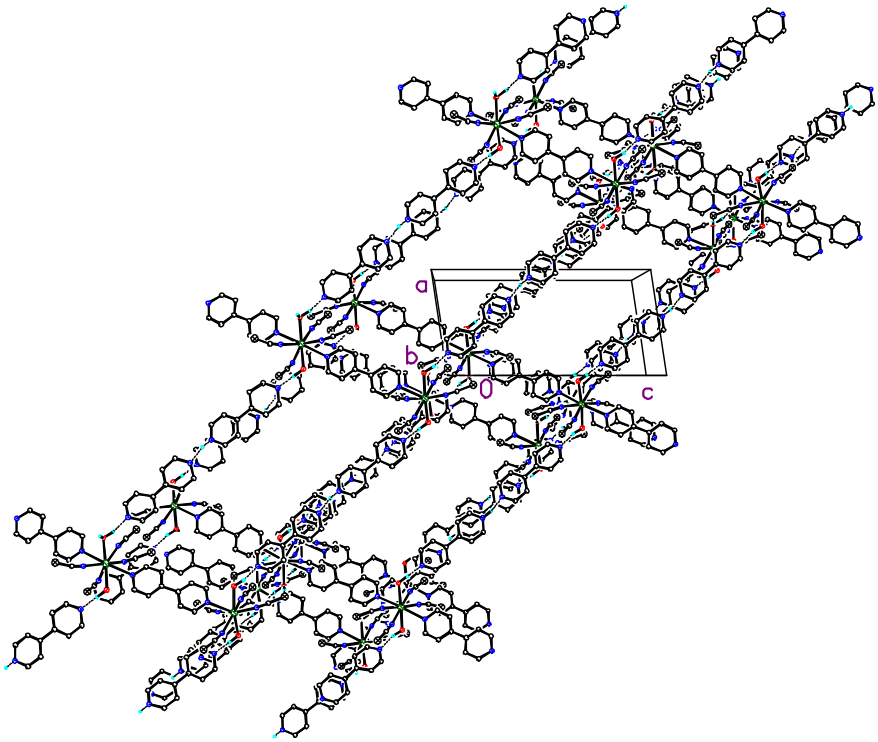

Fig.6. Fragment of structure **6** projected along the b axis**.**

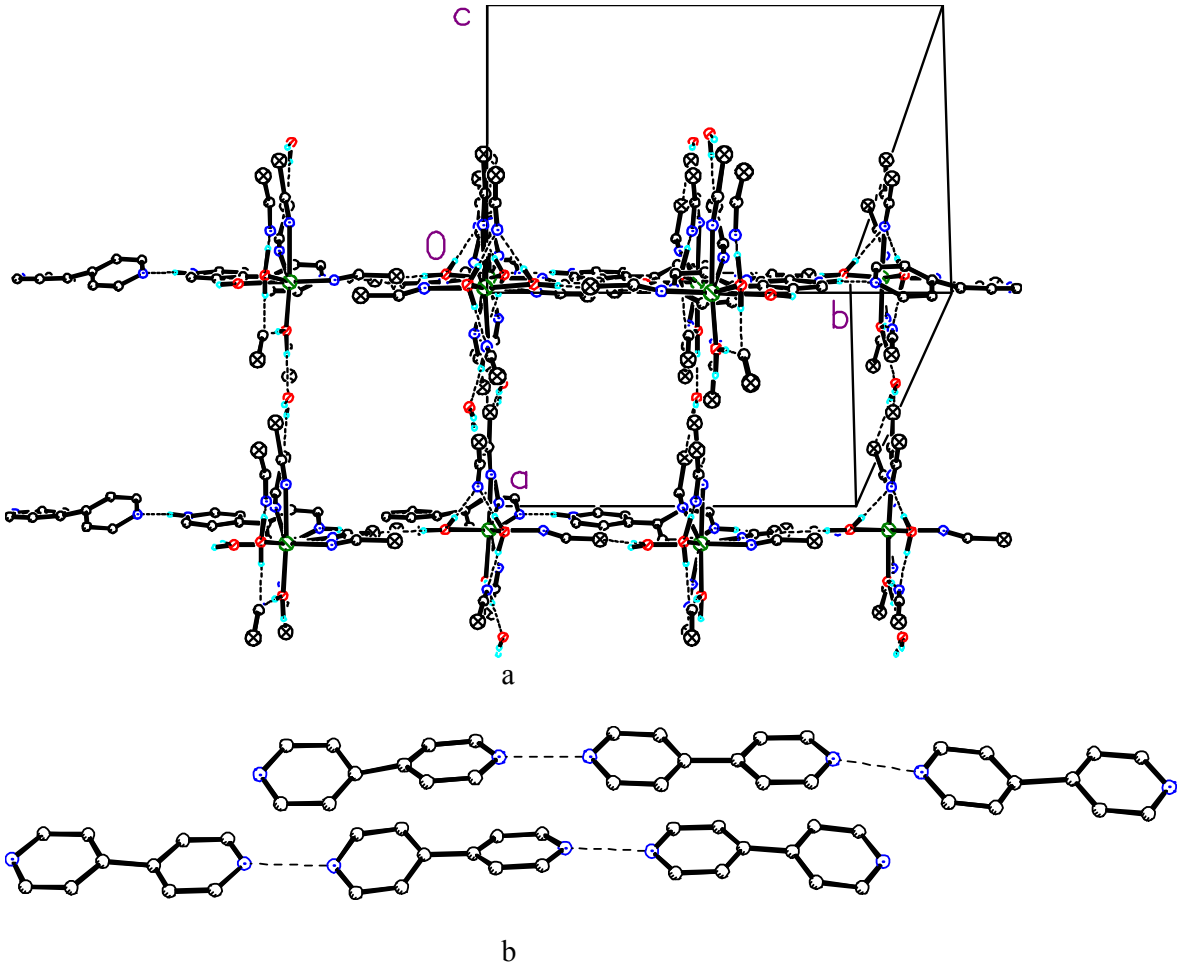

Fig.7. Fragment of structure 7 projected along the [1 0 1] direction (**a**); chains in structure **7 (b).**

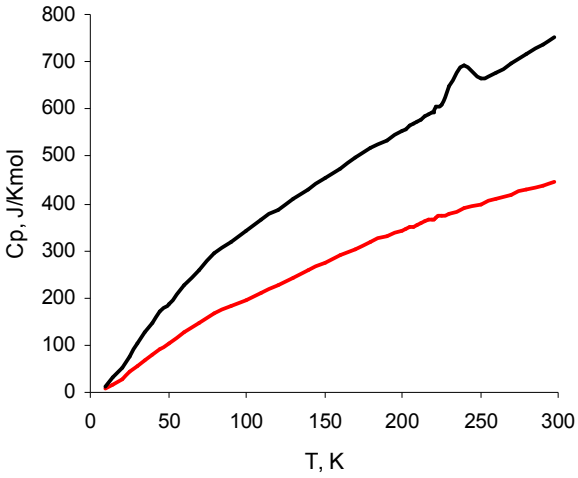

Fig. 8. Temperature dependence of the molar heat capacity of the starting complex $[Y(H_2O)_5(NCS)_3]\cdot H_2O$ (red) and **1** (black)

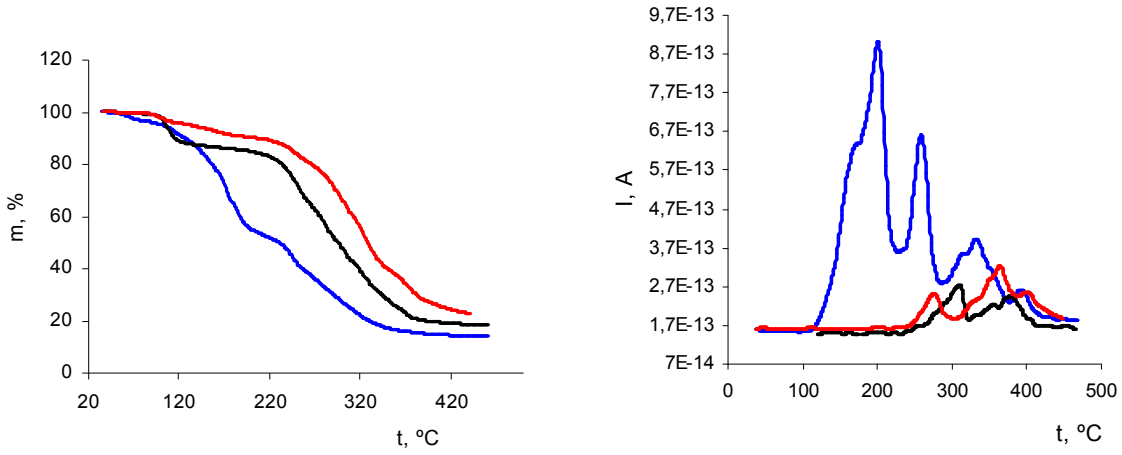

a b

Fig. 9. TG curves (a) and the temperature dependence of the ionic current in the mass spectra of the gases that evolved during thermogravimetry: m/z=156 (b) for compounds: **1** - black; **2** -blue; and **3** - red curves.

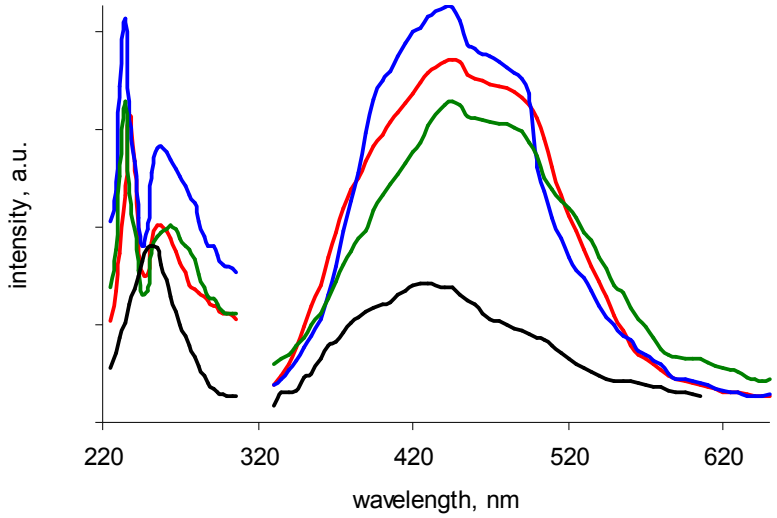

Fig. 10**.** Excitation spectra recorded for the emission band at λ_{reg} = 450 nm (left area) and emission spectra measured using excitation at λ_{exc} = 238 nm (right area): ([$Y(H_2O)_3EtOH(bpy)(NCS)_3$]·bpy (**1**) -blue; {(μ-bpy)[$Y(H_2O)_3(NCS)_3]_2$}·3bpy·2(i-PrOH) (**2**) - red; [Hbpy]$_2${(μ-bpy)[$Y(H_2O)_3(NCS)_4]_2$}·bpy (**3**) - green; [$Y(H_2O)_5(NCS)_3$]·H_2O [7] – black, respectively.